ANALYSIS AND APPLICATION OF OPTO-MECHANICS TO THE ETIOLOGY OF SUB-OPTIMAL OUTCOMES IN LASER CORRECTIVE EYE SURGERY AND DESIGN METHODOLOGY OF DEFORMABLE SURFACE ACCOMMODATING INTRAOCULAR LENSES

by

Sean McCafferty

A Thesis Submitted to the Faculty of the

COLLEGE OF OPTICAL SCIENCE

In Partial Fulfillment of the Requirements

For the Degree of

MASTER OF SCIENCE

In the Graduate College

THE UNIVERSITY OF ARIZONA

2015

STATEMENT BY AUTHOR

This thesis has been submitted in partial fulfillment of requirements for an advanced degree at the University of Arizona and is deposited in the University Library to be made available to borrowers under rules of the Library.

Brief quotations from this thesis are allowable without special permission, provided that an accurate acknowledgement of the source is made. Requests for permission for extended quotation from or reproduction of this manuscript in whole or in part may be granted by the copyright holder.

SIGNED: Sean McCafferty

APPROVAL BY THESIS DIRECTOR

This thesis has been approved on the date shown below:

Jim Schwiegerling
Professor of Optical Science

March 14, 2015
Date

Table of Contents

Figures, Illustrations, and Tables.....5

Abstract.....6

Chapter 1.....10

Introduction.....10

Methods.....14

Results.....18

Conclusions.....22

Chapter 2.....26

Introduction.....26

Methods.....30

Results……31

Conclusions……31

Appendix A – Publication 1……34

Appendix B – Publication 2……35

Appendix C – Publication 3……36

References……...37

List of Figures, Illustrations, and Tables Page

Figure 1- FEA model of contractiing corneal surface……..19

Figure 2- Cross-section of FEA model of contracting corneal surface.....20

Abstract

Overview: Optical concepts as they relate to the ophthalmologic correction of vision in corneal laser vision correction and intraocular lens design was examined.

Purpose: The interaction between the excimer laser and residual corneal tissue in laser vision correction produces unwanted side effects. Understanding the origin of these artifacts can lead to better procedures. Furthermore, accommodating intraocular lenses offer a potential for eliminating presbyopia. Understanding the properties of a new accommodating intraocular lens incorporating a deformable interface may lead to advances in cataract surgery.

Introduction: Corneal surface irregularities following laser refractive procedures are commonly seen. They regularly result in a patient's decreased best corrected visual acuity and decreased contrast sensitivity. These changes are only seen in biologic tissue and the etiology has been elusive. A thermal response has been theorized and was investigated in this research. In addition, intraocular lenses using a mechanically deforming interface to change their power in order to duplicate natural accommodation have been developed. The deforming interface(s) induce optical aberrations due to irregular deformations. Design efforts have centered on minimizing these deformations. Both of the

ophthalmic applications have been analyzed using finite element analysis (FEA) to understand their inherent optical properties.

Methods: FEA modeling of thermal theory has been applied to verify that excimer laser induced collagen contraction creates corneal surface irregularities and central islands. A mathematical model which indicates the viability of the theory was developed. The modeling results were compared to post ablation changes in eyes utilizing an excimer (ArF 193 nm), as well as non-ablative thermal heating in eyes with a CO_2 laser.

Addition modeling was performed on an Intraocular lens prototype measuring of actuation force, lens power, interface contour, optical transfer function, and visual Strehl ratio. Prototype verified mathematical models were utilized to optimize optical and mechanical design parameters to maximize the image quality and minimize the required force.

Results: The predictive model shows significant irregular central buckling formation and irregular folding. The amount of collagen contraction necessary to cause significant surface changes is very small (0.3%). Uniform scanning excimer laser ablation to corneal stroma produces a significant central steepening and peripheral flattening in the central 3mm diameter. Isolated thermal load from uniform CO_2 laser irradiation without ablation also

produces central corneal steepening and paracentral flattening in the central 3mm diameter.

The iterative mathematical modeling based upon the intraocular lens prototype yielded maximized optical and mechanical performance through varied input mechanical and optical parameters to produce a maximized visual Strehl ratio and a minimized force requirement.

Conclusions: The thermal load created by laser irradiation creates a characteristic spectrum of morphologic changes on the porcine corneal stromal surface which correlates to the temperature rise and is not seen inorganic, isotropic material. The highly similar surface changes seen with both lasers are likely indicative of temperature induced transverse collagen fibril contraction and stress re-distribution. Refractive procedures which produce significant thermal load should be cognizant of these morphological changes.

The optimized intraocular lens operates within the physiologic constraints of the human eye including the force available for full accommodative amplitude using the eye's natural focusing feedback, while maintaining image quality in the space available. Optimized optical and mechanical performance parameters were delineated as those which minimize both asphericity and actuation pressure. The methodology combines a multidisciplinary basic science approach from

biomechanics, optical science, and ophthalmology to optimize an intraocular lens design suitable for preliminary trials.

Chapter 1

Introduction:

Modern refractive procedures using Argon-Fluoride (ArF) excimer (λ =193nm) laser radiation to change surface shape of the human cornea have been used successfully for two decades. The procedure is elective with high patient expectations. Often visual outcomes are acceptable to the patient. However, a significant minority of patients have poor or reduced visual outcomes leading to a decrease in best corrected visual acuity (BCVA). One of the major causes in symptomatic patients with poor visual outcomes are linked to corneal aberrations and central island formation.[5,22] It should be noted that poor outcomes can be due to ablation decentration, surgical flap complications, ablation edge aberrations, relative contraindications such as cataracts and corneal disease, and poor ablation quality. The studies presented here look at the often subtle decrease in best corrected visual acuity and contrast sensitivity experienced by most patients who have undergone laser ablative refractive procedures. The incidence of central islands has been reduced through preventative, "over-ablation" of the central cornea included in the software of all commercial lasers, without a clear understanding of its cause.[28,30] This empiric pre-treatment is utilized irrespective of the mode of delivery, broad-beam, flying spot, or scanning slit. It is also utilized irrespective of the procedure, LASIK, PRK, or LASEK.

Several studies have indicated a decreased incidence in central island formation, but fail to indicate the intentional pre-ablation as the cause. [36,37,] Corneal central islands persist despite the use of flying spot laser ablation, which all use a central island pre-treatment.[4] Corneal surface irregularities following laser refractive procedures are commonly seen with various forms of topography. These irregularities include the formation of central islands, spherical aberration, coma, and other higher order aberrations. Commonly used, Placido-based corneal topography often miss mild irregularities of the central cornea (central 1.5mm). The Placido-based topography accurately measures the rate of change of curvature in the radial direction outside the central 1-2 mm of the cornea. Thus, smaller central islands and smaller radial folds, which have a rate of change in curvature predominantly in the circumferential direction, are often missed. Various mechanisms have been proposed independently for the development of each of these irregularities.[1,2,3,7,8,27,28,29,30,31,32,33,34,35] The theoretical model proposed may provide an alternative and productive avenue for future research and directed solutions other than empiric pre-treatment.

Corneal collagen contraction is produced by heating the collagen fibril triple-helix causing it to denature and fold upon itself. Many methods for heating corneal collagen have been developed experimentally and commercially. They include laser radiation, heated filaments, and radiofrequency radiation.
Thermally denatured collagen can shrink between 8% and >30% of its original length.[18] Maximal collagen contraction and denaturation without thermal

necrosis occurs at about 60 degrees celcius.[19,20,21] The human cornea has been shown to be heated to 60 to 70 degrees Celsius during ablation with ArF excimer .[17] This temperature rise is caused by ablation fluences utilized in both broad-beam and flying spot lasers.[31] In addition to heating, collagen contraction following exposure to UVA radiation of riboflavin treated corneas has also been demonstrated.[15]

There is good evidence that collagen fibril tensioning is an active regulated process in the human cornea as evidenced by the constant tension seen across the thickness of the cornea.[16,24] This indicates active tensioning of the outer fibers to maximize the efficiency of the cornea by maintaining a constant stress profile across the thickness of the cornea. If no active tensioning were present, ultimately the stress profile would be maximal on the inner fibers and zero at the outer fibers as seen in thick-walled pressure vessel theory.

The partly transient nature of collagen contraction corresponds to the relaxation time seen in corneal irregularities with the abatement of symptoms in the patient.[9] This initial formation and relaxation of myopic shift and central island formation mimics that seen with *in vivo* collagen denaturation and relaxation. Thermal corneal collagen contraction is utilized in laser thermokeratoplasty (LTK). LTK has fallen out of favor after several iterations due to the subsequent relaxation of the collagen contraction over approximately 6 months following treatment.

Central Islands and hyperopic shift are also shown to “relax” with time mimicking the relaxation seen with known collagen contraction.[10,29,37]

Non-homogeneous ablation profiles have been proposed to explain surface irregularities.[1] Laser calibration techniques have largely eliminated non-homogeneous ablation profiles. Potential aspheric ablations are possible due to decreased fluence and increased reflectivity secondary to the increased angle of incidence seen with increased radial distance from the central cornea.[31,32]Plume interference with the laser delivery to the tissue has also been proposed as a mechanism of central islands, but its abatement, through plume removal, has had little effect on any surface irregularities.[2] Laser pulse-tissue interaction including hydration and acoustic shock waves have also been proposed as a possible cause of surface irregularities.[3,8] Variable epithelial in-growth has also been implicated in transient surface changes seen after ablation in PRK.[27] The same surface irregularities, however, are seen with lasik, suggesting these latter mechanisms are unlikely. Corneal wound healing may also produce corneal deformation and aberrations relatively rapidly, which smooth with time[35] Corneal wound healing, like wound healing elsewhere, may have contractile effects on the ablated surface and could be predicted to behave in a similar fashion as described in this model. However, central islands appear immediately following ablation as do many other aberrations. Unfortunately, these theories have little mathematical support, explain few of the irregularities and have not produced wide-spread support or solutions to central islands and other aberrations seen in

clinical practice. Particularly, the advent of flying spot lasers should have eliminated the mechanisms previously proposed. However, corneal central islands persist with flying spot laser ablation.[4] Other interventions to eliminate the proposed mechanisms have had little effect upon the persistence of central islands.[1,6] Corneal spherical aberration and other higher-order aberrations persist with little explanation, [5] with one possible exception being a comatic aberration induced by a decentered ablation.[7] All commercially produced excimer lasers for refractive surgery include empiric based software to compensate for an anticipated central island despite the many generations of design changes over the last two decades. Even with this software a large percentage of patients will have significant central island formation.[5]

The human corneal stroma, which provides 90% to 95% of the strength of the cornea, is composed of bands of randomly interwoven lamellae.[23,26] There are between 300-400 lamellae across a representative thickness of the cornea. Each lamellar band is approximately 2 micrometers in thickness, 2 to 3mm wide, and extends in random orientations from limbus to limbus. Each lamellae has 25 nanometer diameter fibers in hexagonal close pack cross-sectional orientation set in ground substance on 62 nanometer centers. There is no interdigitation of fibrils from adjacent lamellae.[12]

Methods:

An advanced finite element model (Algor, V23, Pittsburg, PA) was constructed based upon the lamellar structure of the cornea. Surface stromal collagen contraction was modeled to only to look at changes in profilometry from a previously spherical surface. Also, 100 microns and 200 microns of uniform corneal thinning were modeled. A lamellar composite was used to model the stroma of the cornea. The stromal collagen was modeled as layers of thin membrane elements extending from limbus to limbus. The membrane collagen layers show resistance to tension only, not compression or shear. Between each collagen lamellae is a ground substance layer constructed of brick elements, which maintains isotropic properties including a greatly reduced Young's and Shear modulus of elasticity. Lamellar boundaries were maintained and adjacent elements in overlying lamellae were fused. Effectively the model exhibits great strength in tension, tangential to the corneal curvature. It has little strength in compression or bending. Also, there is relatively little resistance to shear between the lamellae. Construction of the model in this manner effectively emulates the properties of the cornea seen experimentally and clinically.

The collagen lamellae's modulus of elasticity (Young's) was input at 1.0 GPa. Both the Young's and shear modulus for the ground substance were input at 10^{-5} GPa.[25] A linear modulus of elasticity was used in development of the model which has good support for forces and displacements in the physiologic range.[12,13,14] A standard spherical (radius = 7.8mm, diameter=11.5mm) cornea

of uniform thickness (600 micrometers) was utilized. Boundary elements were used at the corneal edge to simulate adjacent sclera. The thickness of the elements in each lamellae model the amount collagen verses ground substance seen in experiment, approximately 2-3% collagen fibril.[23,26] Standard intraocular pressure of 16 mm Hg was used. Pre- tensioning of the outer fibers of the cornea was modeled by varying the stiffness of the boundary elements along the thickness of the cornea. This would give a physiologic, uniform stress distribution across the thickness of the cornea in the pre-contracted state.[16]

Force elements were used to form a uniform disk of contraction over a central 6mm ablation zone. The following equation was used to determine the amplitude of the force at any given radial distance. It was developed by assuming that all areas contracting on the disk pull toward each other equally. The formula was derived by assuming a uniform flat disk in which all points are “pulled” toward all other points on the disk proportional to their distance and direction. This would be similar to the gravitational pull experienced by a uniform disk of mass, at any point within the disk. Due to symmetry, only the radial position needs to be considered.

$$Ar(unit\ force\ at\ radial\ position\ r) = 1 - \frac{\frac{R^2}{2}\left(2\cos^{-1}\frac{r}{R} - \sin\left(2\cos^{-1}\frac{r}{R}\right)\right)}{\pi R^2 - \frac{R^2}{2}\left(2\cos^{-1}\frac{r}{R} - \sin\left(2\cos^{-1}\frac{r}{R}\right)\right)}$$

The center would have zero force and maximal force would be seen at the radius= 3mm. Forces along the radius would be proportional to the area of the

larger segment of the disk divided by the total area of the disk. The vector of the nodal force was assumed to be centripetal and tangential to the corneal surface through the node. Non-uniform contractions were modeled by varying the percentage of contractile force over the angular position of the node (theta).

Numerous other methods were utilized and are outlined in detail in the previously published articles. Refer to Appendices A and B for details, but the basic outline of the methods are noted here:

Appendix A methodology - Ten (10) cadaveric porcine eyes with exposed corneal stroma and plastic test spheres underwent uniform 6mm ablation using a Visx S4 scanning excimer laser. Corneal profilometry of the central 3mm was measured with sub-micron resolution optical interferometry before and after uniform excimer ablation. Eleven (11) surface marked eyes were photomicrographed before and after excimer ablation. Images were superimposed and mark positional changes were measured.

Appendix B methodology - Cadaveric porcine eyes were pressurized and stabilized for processing and imaging. Both a scanning excimer laser and a CO_2 laser were used to deliver a uniform disk of radiant energy to the exposed corneal stromal surface. Thermal load was determined by measuring corneal surface temperature during irradiation. Corneal profilometry was measured with broad-band optical interferometry before and after laser irradiation.

Photomicrographs of the stromal surface were taken before and after irradiation and the images were superimposed to examine changes in positional marks examining mechanical alterations in the stromal surface.

Results:

Uniform collagen contraction on the surface of the ablated cornea, shown using the finite element analysis (FEA) model, causes irregular central island formation (Figure 3). The contraction also induces paracentral flattening. This is shown in Figure 1 with the deformed model average radial profile from a previously spherical surface (averaging circumferential peaks and valleys). Any non-uniformity of the model's collagen contraction would also induce an irregular astigmatic deformation central island as shown in Figure 2. Alternatively, any weakness of the cornea or segmental thinning would cause radial buckling in the direction(s) of the weakness, even if the collagen contraction was uniform.

Figure 1 – FEA model of contractiing corneal surface.

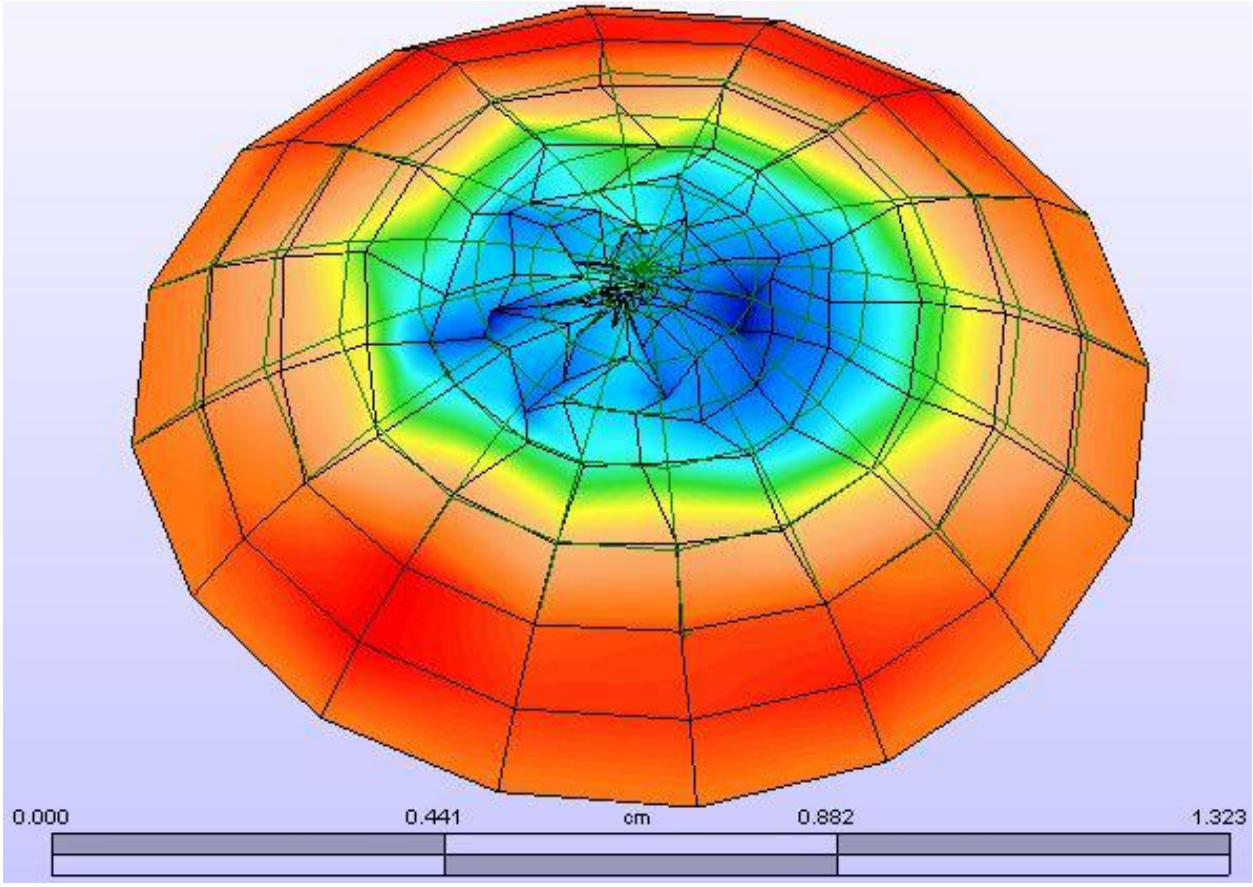

Figure 2 – Cross-section of FEA model of contracting corneal surface, showing paracentral flattening and central steepening.

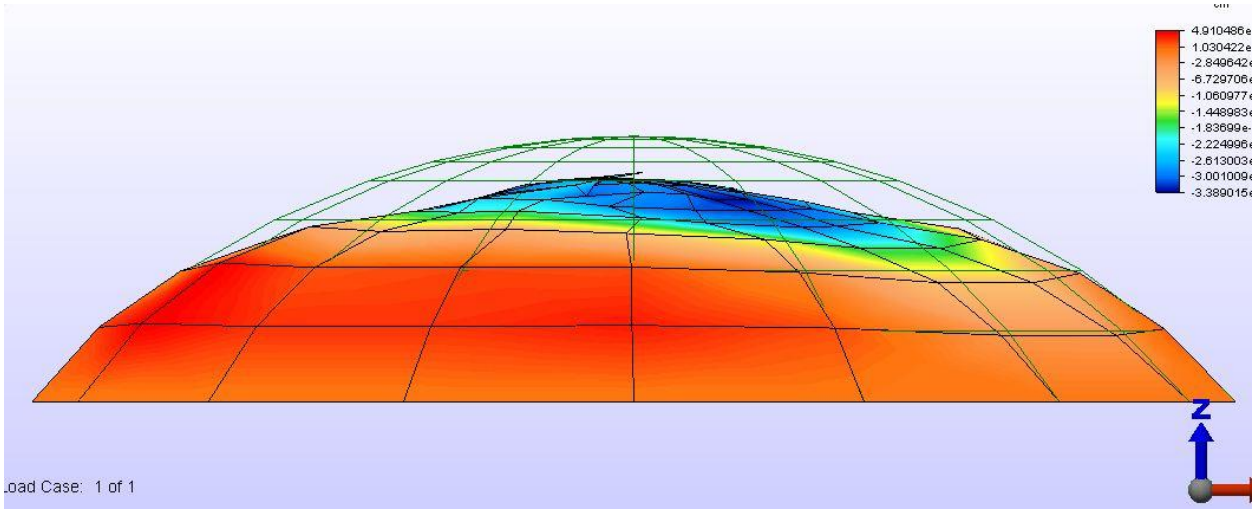

A superficial skin depth stromal collagen contraction is presented in Figures 1 and 2. However, as the cornea becomes thinner as would occur with increased laser ablation depth, only the amplitude of the presented aberrations increases moderately. The surface profilometry patterns remain the same as those presented. Amplitudes of the model's deformations increase to 12% and 26% with 100 and 200 microns of the corneal stroma removed, respectively.

The irregular petaloid pattern of the radial buckling will occur in any rosette pattern depending upon areas of comparative weakness or thinning across the cornea. This could lead to a single area of buckling if there is a prominent area of corneal weakness or an astigmatic "ridge" as shown in figure 1. The amount of collagen contraction necessary to produce all of the irregularity patterns shown is 0.3% of the irradiated surface.

Numerous other results were obtained and are outlined in detail in the previously published articles. Refer to Appendices A and B for details, but the basic outline of the results are noted here:

Appendix A results - Uniform scanning excimer laser ablation to corneal stroma produces a significant central steepening and peripheral flattening in the central 3mm diameter. The central 1mm corneal curvature radius decreased from r=10.07+/-0.44mm(95%CI) to 7.22+/-0.30mm and the central 2mm radius decreased from r=10.16+/-0.44mm to r=8.10+/-0.43mm. Q-values, measuring asphericity in the central 2mm of the cornea, were significantly lower pre-ablation than post ablation (-5.03+/-4.01vs.-52.4+/-18.7,respectively). Surface roughness increased significantly from 0.65+/-0.06microns to 1.75+/-0.32microns following ablation. The central 2mm of the stromal surface contracted by 2.21%+/-0.80% at a sustained temperature of 5°C. Ablation of plastic spheres produced no significant changes.

Appendix B results - Isolated thermal load from uniform CO_2 laser irradiation without ablation also produces central corneal steepening and paracentral flattening in the central 3mm diameter. Q-values, measuring asphericity in the central 2mm of the cornea increased significantly and it was correlated with the temperature rise (R^2=0.767). Surface roughness increased significantly and was also correlated with temperature rise (R^2=0.851). The central stromal surface

contracted and underwent characteristic morphologic changes with the applied thermal load which correlated well with the temperature rise (R^2=0.818).

Conclusions:

The excimer laser (ArF) causes corneal surface irregularities and central islands through skin-depth corneal collagen contraction created by the brief temperature rise. The presented research introduced this new theory and explored its mechanism in explaining induced surface irregularities and central island formation following excimer laser corneal refractive procedures. It should be noted that poor outcomes can be due to ablation decentration, surgical flap complications, ablation edge aberrations, relative contraindications such as cataracts and corneal disease, and poor ablation quality. The studies presented examine the often subtle decrease in best corrected visual acuity and contrast sensitivity experienced by most patients who have undergone laser ablative refractive procedures.

A finite element model was constructed based upon the lamellar structure of the cornea. Corneal stromal surface collagen contraction was modeled to predict changes in surface profilometry from a previously spherical surface with minimal corneal irradiation. The mathematical model showed central corneal irregularities with island formation and radial folding, creating a multitude of surface irregularities. Another recent study has shown very similar morphologic

changes in differential contraction in biologic lamellar sheets adding to the body of evidence supporting this contraction theory.[49]

The excimer laser interacts with the unablated residual stromal surface in a characteristic fashion not seen with isotropic, inorganic material. Increases in asphericity, surface roughness, surface contraction, and stromal morphological changes are supportive of this interaction. The interaction is very similar to the changes predicted in the FEA mathematical model. The surface changes demonstrated may be indicative of temperature induced transverse collagen fibril contraction and stress re-distribution or the ablation threshold of the stromal surface may be altered.

A CO_2 laser was constructed and used as a known collagen thermal denaturing agent to irradiate the surface of the corneal stroma. The CO_2 laser effectively recreated central islands and other corneal surface irregularities predicted by the finite element model and also seen in the excimer laser ablation.

A Three (3) phase theory verification that corneal excimer laser ablation induces collagen contraction and creates corneal surface irregularities and central islands was completed as follows:

1. A mathematical model was developed which indicates the viability of the theory and expected behavior.
2. A known thermal collagen contracting agent without tissue ablation was used on the cornea and surface changes were measured with comparison to the mathematical model.
3. The excimer (ArF 193nm) laser was used to ablate the corneal surface and was compared to that of the CO_2 laser thermal irradiation and the model. A very similar morphology in corneal surface changes to that produced by the continuous CO_2 laser induced collagen contraction indicates that thermal collagen contraction is the likely etiology for these changes.

The theory and supportive studies attempt to answer the 20 year old question of central island formation in addition to tying together many clinically observed surface irregularities following corneal excimer ablation. Further studies in human cadaveric eyes and in-vivo clinical studies able to measure the central stromal corneal surface would be desirable for theory verification.

There is a threshold temperature at which collagen contraction accelerates rapidly. It appears that the formation of central corneal irregularities is likely a function of temperature rise due to pulse duration, and laser fluence. There also is likely some role in the laser pulse frequency to the same area, thus increasing the temperature of that area beyond the contraction threshold. It is possible to

prevent the formation of excimer induced surface irregularities by varying the mentioned parameters or real-time monitoring of corneal surface temperature. Interventions to the proposed mechanism could maintain a threshold temperature below a critical value, leading to better outcomes in laser vision correction.

Chapter 2

Introduction:

Natural accommodation is the eye's ability to change the shape of its lens and thereby change its focal distance. This allows an individual to focus on objects over a continuous range of distances in their view with an autonomic nervous system feedback response. The person does this automatically, without thinking, by innervating their ciliary body muscle in the eye. The ciliary muscle adjusts radial tension on the natural lens and changes the lens' surface curvatures leading to a change in the focal distance of the eye.[38]

Without the ability to accommodate, lenses such as reading glasses must be relied upon to focus on desired objects. The normal aging process causes a steady reduction in accommodation, leading to presbyopia around the age of 50. Furthermore, traditional cataract surgery ensures a loss of accommodation since conventional intraocular lenses (IOLs) have a single refractive power and are fixed within the eye. Cataract surgery typically targets a mildly myopic post-operative refractive that will leave the individual with a fixed focal distance, typically greater than 20 feet. This allows them to function in activities such as driving without glasses. For activities such as computer work or reading, they

need separate glasses to provide the additional power required to bring objects at these distance into focus.[39]

A variety of techniques have been explored to alleviate the lack of accommodation following cataract surgery. The most successful of these rely upon multifocal IOLs, which are lenses with multiple focal lengths that provide in-focus images to the retina at several discrete planes. Multifocal optics rely on simultaneous vision, meaning that both in-focus and out-of-focus images are presented simultaneously and the visual cortex needs to learn to ignore the blurry information and extract the sharp information. These lenses inherently reduce contrast in the retinal image and degrade overall quality of the vision when compared to the continuous quality of natural accommodation.[40] Accommodating IOLs are an emerging class of implants that attempt to restore accommodation by enabling the focal distance of the eye to change. Early versions of accommodating IOLs relied upon axial translation of the implant to change its position (and the overall power of the eye) relative to the cornea. These technologies have performed poorly in clinical application and are limited in the degree of power change that can be achieved. Newer concepts of continuously accommodating IOL's incorporating a shape changing interface have been demonstrated. The Nulens concept utilizes the radial tension provided by relaxation of the ciliary muscle to provide an anterior vectored force on the lens allowing it to alter the curvature of the lens' interface and the overall lens power.[41,42] The IOL concept uses the anterior vectored force to extrude a

high index refraction gel material through a rigid circular aperture which deforms in a more or less spherical shape. The increasing spherical deformation creates a lens of increasing power and is directly proportional to the force applied to it. One probable drawback to this design is that the autonomic feedback is reversed from natural accommodation. Ciliary muscle contraction in this case causes a decrease in lens power focusing the eye at a more distant object instead of natural accommodation which is the other way around.

We have developed an alternative version of the extruded gel interface lens that accommodates in the proper direction. Our extruded gel accommodating lens (EGAL) incorporates a bicameral chamber separating a gel material in the posterior chamber of lower index of refraction and an anterior fluidic chamber of higher refractive index. The fluid in the anterior chamber has higher refractive index than the gel in the posterior chamber. When the gel interface is extruded through the internal rigid aperture, it reduces the overall power of the lens.[43] The outer shell is a continuous material between the haptics and the anterior surface of the lens. This “buttressed” dome shape of the haptics is able to maximally transfer the pressure applied the posterior surface of the lens out to the anchor points of the haptics seated in the sulcus of the eye. The tissue (ciliary body, zonules, and capsule) overlying the dome shape buttresses the haptics and lens which prevents buckling and increases stiffness while still able to be made from an easily insertable foldable acrylic material (see Fig. 1).

The EGAL is an azimuthally symmetric design. Continuity minimizes glare due to light scatter and diffraction. The accommodating IOL design incorporates a posterior flexible gel (Silicone or Slygaard^{TM}) and an anterior chamber of silicone oil or glycerin separated by rigid poly methyl methacrylate (PMMA) plate with an extrusion aperture to allow the spherical change in power as pressure provided by the ciliary muscle pushes the gel through the aperture. The entire design is contained in a rigid acrylic or PMMA shell which is continuous with the haptics. The anterior vectored force created by the zonule/capsular tension to pressurizes the posterior gel. Increased pressure in the posterior chamber deforms the flexible interface in a more or less spherical shape and decreases the overall power of the lens.

The posterior surface of the lens would be that of a spherical lens. When the ciliary muscle is relaxed (during distance focusing of the eye), tension is increased on the zonules and the lens capsule similar to the tightening of a drum head. Increasing tension on the lens capsule applies an anterior vectored force on the posterior surface of the lens which is displacing the capsular membrane posteriorly. This applied pressure will anteriorly displace the posterior lens acting as a piston to pressurize the posterior gel and spherically deform the inter-chamber interface anteriorly. The higher refractive index in the anterior chamber compared to the posterior chamber will effectively decrease the power of the whole lens system in direct proportion to the posterior applied pressure. This effect will be equivalent to reduction in the overall power of the lens just as the natural lens in an eye relaxes accommodation to focus on a distant object.[38]

Conversely, during accommodation the ciliary muscle contracts relaxing the tension on the zonules and the capsular membrane. The relaxed tension decreases the pressure on the posterior surface of the lens allowing it to resume its unstressed spherical shape. This in effect increases the power of the lens just as the natural lens does during accommodation to focus on a near object.

One major potential drawback to any mechanical design for an accommodating IOL is the small force applied by the capsular membrane (about 1 gram) which must be sufficient to actuate the lens and alter its shape and power.[44] The second potential drawback is the inherent asphericity of an extruded gel interface creating poor image quality. The present study attempts to delineate the factors affecting force and image quality in opto-mechanical design of an extruded gel accommodating lens (EGAL). Performance of intraocular lenses has been measured the optical transfer function (OTF), the visual OTF, and the visual Strehl ratio.[45,46,47,48]

Methods:

Appendix C methodology - The next generation design of extruded gel interface intraocular lens is presented. A prototype based upon similar previously in-vivo proven design was tested with measurements of actuation force, lens power, interface contour, optical transfer function, and visual Strehl ratio. Prototype

verified mathematical models were utilized to optimize optical and mechanical design parameters to maximize the image quality and minimize the required force to accommodate.

Results:

Appendix C results - The prototype lens produced adequate image quality with the available physiologic accommodating force. The iterative mathematical modeling based upon the prototype yielded maximized optical and mechanical performance through: Maximum allowable gel thickness to extrusion diameter ratio. Maximum feasible refractive index change at the interface. Minimum gel material properties in Poisson's ratio and Young's modulus.

Conclusions:

An accommodating intraocular lens incorporates an extruded internal gel to create an interface of increasingly negative power with physiologic pressure provided by relaxation of the ciliary body muscle. The optimum design attempts to produces a nearly spherical interface to minimize aberrations. A deformed solid cannot create a truly spherical surface and instead produces and oblate asphere. As a result the aspheric aberrations create a broadening of the

incoherent point spread function (PSF) and a decrease in the image quality. This is seen by patients as decreased visual acuity and contrast sensitivity.

The prototype performed within the physiologic constraints of the human eye. The parameters which optimized optical and mechanical performance were delineated as those which minimize asphericity and actuation pressure. Identified design parameters can be used as a template to maximize the performance of any deformable interface intraocular lens. The natural force available from the eye's ciliary body muscle contraction and zonular/capsular tension is minimal. Therefore any design must incorporate a minimal force required to actuate the lens while not exceeding its elastic limits.

Important design parameters not examined in this study would include: Biocompatibility of the material in inflammation and material property stability. Its ability to pass through a small incision in the eye. Minimal refractive discontinuities in the lens optic to minimize scatter. Lens anchoring system exhibiting stability and able to actuate lens and prevent creep and migration through tissue. Ability to utilize pupillary meiosis during actuation for near focus. Posterior capsular opacification. The need for extruded gel displacement of the incompressible anterior liquid to expand elsewhere.

The optimization methodology outlined here can be extrapolated to the design of any deformable interface intraocular lens. The method takes a basic concept to produce a 'best guess' prototype. It then incorporates a mathematical model based upon the prototype's optical, mechanical, and ophthalmic properties to

optimize the design. Optimization involves varying the input design properties to produce maximized merit output functions, in this case: maximum visual optical quality and minimum actuation force. The optimized design is then able to be used in initial animal implantation studies and as a basis for further revision based upon those in-vivo trials.

Appendix A

PDF of publication can be loaded directly from this URL:

http://iovs.arvojournals.org/article.aspx?articleid=2188265

Appendix B

PDF of publication can be loaded directly from this URL:

http://iovs.arvojournals.org/article.aspx?articleid=2130013

Appendix C

PDF of publication can be loaded directly from this URL:

http://tvst.arvojournals.org/article.aspx?articleid=2288835&resultClick=1

References

1. Fantes FE, Warning GO III. Effect of excimer laser radiant exposure on uniformity of ablated corneal surface. Lasers Surg med 1989; 9:533-544.

2. Noack J, Tonnies R, Hohla K, et al. Influence of ablation plume dynamics on the formation of central islands in excimer laser photorefractive keratectomy. Ophthalmology 1997; 104:823-830

3. Dougherty PJ, Wellish KL, Maloney RK. Excimer laser ablation rate and corneal hydration. Am J Ophthalmol 1994; 118:169-176

4. Muller B, Thomas B, Hartmann C. Effect of excimer laser beam delivery and beam shaping on corneal sphericity in photorefractive keratectomy. J Cataract refract surg 2004; 30:464-470

5. McCormick G, Porter J, Cox I, MacRae S. Higher-Order Aberrations in Eyes with irregular Corneas after Laser Refractive Surgery. American Academy of Ophthalmology 2005; 1699-1709

6. Itoi M, Ryan R, Depaolis M, Aquavella JV. Clinical effect of blowing nitrogen gas across the cornea during photorefractive keratectomy. J refract Surg 1997; 13:69-73

7. Mrochen M, Kaemmerer M, Mierdel P, Seiler T. Increased higher-order optical aberrations after laser refractive surgery; a problem of subclinical decentration. J Cataract Refract Surg 2001; 17:608-612

8. Oshika T, Klyce SD, Smolek MK, McDonald MB. Corneal hydration and central islands agter excimer laser photorefractive keratectomy. J Cataract Refract Surg 1998;12:1575-1580

9. Abbas UL, Hersh PS. Early corneal topography patterns after excimer laser photorefractive keratectomy for myopia. J of refra surgery 1999; 15:124-131

10. Kang S, Chung E, Kim W. Clinical analysis of central islands after laser in situ keratomileusis 2000; 26: 536-542

11. Fisher B. Investigation on interactions between the 193 nm argon-fluride excimer laser and corneal tissue. DAI-B 2005; 65/12:6612

12. Pinsky PM, Datye DV. A microstructurally-based finite element model of the incised human cornea. J Biomechanics 1991; 24: 907-922

13. Zeng Y, Yang J, Huang K, Lee Z, Lee X. A comparison of biomechanical properties between human and porcine cornea. J of biomechanics 2001; 34: 533-537

14. Woo S, Kobayashi AS, Schlegel WA, Lawrence C. Nonlinear Material Properties of Intact Cornea and Sclera. Exp Eye Res 1972; 14:29-39

15. Wollensak G, Spoerl E, Seiler T. Stress-strain measurements of human and porcine corneas after riboflavin-ultraviolet-A-induced cross-linking. J cataract refract surg 2003; 29:1780-1785

16. McPhee, T.J., Bourne W.M. and Brubaker, RF. Location of stress bearing layers of the cornea. Invest Ophthalmol Vis Sci. 1985; 26: 869-872

17. Ishihara M, Arai T, Sato S, Morimoto Y, Obara M, Kikuchi M. Temperature measurement for energy efficient ablation by thermal radiation with a microsecond time constant from the corneal surface during ArF excimer laser ablation. Frontiers of medical & biological engineering 2001; Vol. 11 Issue 3: 167-175

18. Ross V, Yashar S, Naseef G, Barnette D, Skrobal M, Grevelink J, Anderson R. A pilot study of in vivo immediate tissue contration with co₂ skin laser resurfacing in a live farm pig. Dermatologic Surgery 1999; Vol 25 issue 11: 851-856

19. Xu f, Wen T, Seffen KA, Lu TJ. Characterization of thermomechanical behavior of skin tissue I Tensiloe and Compressive behaviours. World Congress on Engineering 2007; 2:1446-1450

20. Sionkowska A. Thermal stabiliry of Uv-irradiated collagen in bovine lens capsules and in bovine cornia. J of Photochemistry & Photobiology B: Biology 2005; Vol 80 issue 2: 87-92

21. Rossi F, Pini R, Menabuoni Luca. Experimental and model analysis on the temperature dynamics during diode laser welding of the cornea. J of Biomedical Optics 2007; Vol 12 Issue 1:14031-14031

22. Krueger R, Saedy N, McDonnell P. Clinical Analysis of steep central islands agter excimer laser photorefractive keratectomy.Arch Ophthalmol 1996;114: 377-381

23. Kamai Y, Ushiki T. The Three-Dimensional Organization of Collagen Fibrils in the Human Cornea and Sclera. Investigative Ophthal &Vis Sci 1991; 32-8:2244-2258

24. Eliason J, Maurice DM. Stress Distribution across the in vivo human cornea. Invest Ophthalmol Vis Sci 1981; 20:156

25. Jue B, Maurice DM. The mechanical properties of the rabbit and human cornea. J Biomechanics 1986; 10: 847-85326. Maurice, DM. The cornea and aclera. The eye 1984

26. Maurice, DM. The cornea and sclera. The eye 1984

27. Gauthier CA, Epstein D, Holden BA, et al. Epithelial altertions following photorefractive keratectomy for myopia. J Refract Surg 1995; 11: 113-118.

28. Roberts C. Biomechanics of the Cornea and Wavefront-guided Laser Refractive Surgery. J Refract Surg 2002; 18:S589-592.

29. Jabbur NS, Sakatani K, O'Brien TP. Survey of complications and recommendations for management in dissatisfied patients seeking a consultation after refractive surgery. J Cataract Refractive Surgery 2004; Vol 40: 1867-1874

30. Hafezi F, Janko M, Mrochen M, Wullner C, Seiler T. Customized ablation algorithm for the treatment of steep central islands after refractive laser surgery. J Cataract Refract Surg 2006; 32: 717-721

31. Mrochen M, Seiler T. Influence of Corneal Curvature on Calculation of Ablation Patterns Used in Photorefractive Laser Surgery. J of Refractive Surgery 2001; 17: S584-S587

32. Jimenez JR, Anera RG, Jimenez del Barco L, Hita E. Effect of laser-ablation algorithms of reflection losses and nonnormal incidence on the anterior cornea. Appl Phys Lett 2002; 8: 1521-1523

33. Ang EK, Couper T, Dirani M, Vajpayee RB, Franzco, Baird PN. Outcomes of laser refractive surgery for myopia. J Cataract Refract Surg 2009; 35: 921-933

34. Roberts C. The Cornea is not a piece of plastic. J of Refractive Surg 2000; 16: 407-413

35. Huang D, Tang M, ShekharR. Mathematical model of corneal surface smoothing after laser refractive surgery. Am J Ophthalmol. 2003;135:267-278.

36. Torres R, Ang RT, Azar DT. Lasers in Lasik ; basic aspects. Surgical Techniques and Complications 2003; 39-56

37. Seiler T, McDonnell PJ. Excimer laser photorefractive keratectomy. Surv Ophthalmology 1995; 40: 89-118

38. Kaufman FL, Alm A, Adler FH: Adler's physiology of eye: clinical application, 10th Ed. St Louis: Mosby, 2003.

39. Duane's Clinical Ophthalmology. New York: Lippincott Williams & Wilkins, 2005

40. Bohórquez V, Alarcon R. Long-term reading performance in patients with bilateral dual-optic accommodating intraocular lenses. J Cataract Refract Surg 2010;3611:1880-6.

41. Alio JL, Ben-nun J, Rodriguez-Prats J, Plaza AB. Visual and accommodative outcomes one year after implantation of an accommodating intraocular lens based on a new concept. J Cataract Refract Surg 2009;35:10:1671-78.

42. Ben-nun J, Alio JL. Feasibility and development of a high-power real accommodating intraocular lens. J Cataract Refractive Surg 2005; 31:1802-1808.

43. Schwiegerling J, Savidis N, McCafferty SJ. Curvature Changing Accommodating IOL- ARVO presentation, May 10, 2012, 12:00 PM -12:15 PM.

44. Augusteyn RC, Ashik M, Nankavil D, Veerendranath P, Arrieta E, Taneja M, Manns F, Ho A, Parel J. Age-dependence of the optomechanical responses of ex vivo human lenses from india and the USA, and the force required to produce these in a lens stretcher: The similarity to in vivo disaccommodation. Vision Research 2011 vol. 51 pp. 1667-78.

45. Rawer R, Stork W, Spraul CW, Lingenfelder C. Image quality of intraocular lenses. J Cataract Refractive Surg; 2005; 31:1618-1631.

46. Johnson, G. M., Fairchild, M. D. (2002, April) On contrast sensitivity in an image difference model. IS and TS PICS CONFERENCE (pp. 18-23) Society for Imaging Science and Technology.

47. Movshon JA, Kiorpes L. Analysis of the development of spatial contrast sensitivity in monkey and human infants. J Optical Society of America 1988 Dec; Vol. 5(12), pp.2166-72.

48. Young LK, Love GD, Smithson HE. Accounting for the phase, spatial frequency and orientation demands of the task improves metrics based on the visual Strehl ratio. Vision Research 2013, Jul 19.

49. Efrati E, Klein Y, Aharoni H, Sharon E. Spontaneous buckling of elastic sheets with a prescribed non-Euclidean metric. Physica D 235 (2007) 29–32